J Mater Sci: Mater Electron (2014) 25:1404–1409
DOI 10.1007/s10854-014-1742-4

Effects of growth temperature on electrical and structural properties of sputtered GaN films with a cermet target

Cheng-Che Li · Dong-Hau Kuo

Received: 19 December 2013 / Accepted: 16 January 2014 / Published online: 24 January 2014

Abstract GaN films have been deposited at 100–400 °C substrate temperature on Si (100) and sapphire (0001) substrates by RF reactive sputtering in an (Ar + N_2) atmosphere. A (Ga + GaN) cermet target for sputtering was made by hot pressing the mixed powders of metallic Ga and ceramic GaN. The effects of substrate temperature on the GaN formation and its properties were investigated. The diffraction results showed that GaN films with a preferential (10–10) growth plane had a wurtzite crystalline structure. GaN films became smoother at higher substrate temperature. The Hall effect measurements showed the electron concentration and mobility were 1.04×10^{18} cm^{-3} and 7.1 cm^2 V^{-1} s^{-1}, respectively, for GaN deposited at 400 °C. GaN films were tested for its thermal stability at 900 °C in the N_2 atmosphere. Electrical properties slightly degraded after annealing. The smaller bandgap of ~3.0 eV is explained in terms of intrinsic defects and lattice distortion.

1 Introduction

In the recent years, wide bandgap (E_g) III–V nitride semiconductors such as GaN had been applied in light emitting diodes (LEDs) and laser diodes (LD) [1, 2]. GaN had a direct E_g of 3.4 eV and had other excellent characteristics such as thermal conductivity, high breakdown voltage, and high mobility [3]. GaN also could be applied to field-effect transistor (FET) and heterojunction bipolar transistor (HBT) [4, 5]. So far, there are several methods to grow GaN films such as metal–organic chemical vapor deposition (MOCVD), metal–organic vapor phase epitaxy (MOVPE) [6–8]. For MOCVD and MOVPE processes, GaN films have been deposited at 1,000 °C with N_2 as a carrier gas and trimethylgallium (TMG) and ammonia (NH_3) as Ga and N sources, respectively. However, high manufacturing cost and process temperature are the major challenges for MOCVD process.

In addition, sputtering technique was another method to grow GaN films. Sputtering can be divided into direct current (DC) and radio-frequency (RF) sputtering [9]. The sputtering technique had many advantages such as lower deposition temperature than MOCVD, low equipment cost, and secure working atmosphere (Ar, O_2 and N_2). Until now, GaN films have been successful deposited on Si substrate by sputtering. Zhang et al. [10] deposited GaN films on *p*-type Si (111) substrates at 500 °C by DC sputtering with a Ga target in pure nitrogen atmosphere. Kim deposited GaN films on ZnO/Si (001) substrates by RF sputter system with a GaN target in pure Ar atmosphere [11]. Optical and structural properties have been frequently mentioned in the previous reports. However, most reports about electrical properties of GaN films were deposited by MOCVD. Nakamura [6] observed that the carrier concentration and mobility of GaN films were 4×10^{16} cm^{-3} and 600 cm^2 V^{-1} s^{-1}, respectively.

In this work, GaN films have been deposited by a RF reactive sputtering technique. We use the cermet concept to fabricate the (Ga + GaN) cermet target to overcome the problems of using a viscous Ga solid as the sputtering target and sintering a dense target of GaN with a high melting temperature of >2,500 °C. This cermet target was made by hot pressing the powder mixture of 30 vol% metallic Ga and 70 vol% ceramic GaN. The Ga content in

C.-C. Li · D.-H. Kuo (✉)
Department of Materials Science and Engineering, National Taiwan University of Science and Technology, Taipei 10607, Taiwan
e-mail: dhkuo@mail.ntust.edu.tw

target is less than the GaN content to avoid the outflow of viscous Ga during hot pressing and sputtering. Therefore, the GaN films grown at different substrate temperatures with this technique are investigated for its feasibility and growth characteristics.

2 Experimental details

The GaN films were deposited on Si (100) and sapphire (0001) substrates by the RF reactive sputtering technique. The (Ga + GaN) cermet target was made by hot pressing the mixture powder of 70 vol% ceramic GaN and 30 vol% metallic Ga. Before sputtering, the chamber was pumped down to a pressure lower than 1×10^{-6} torr to avoid the impurities, e.g. oxygen. The substrates were heated at 100–400 °C and the sputtering proceeded under the gas mixture of Ar and N_2. Both Ar and N_2 flow rates were set at a flow rate of 5 cm^3/min for each. The sputtering power and deposition time was 120 W and 90 min, respectively. The working pressure was kept at 9×10^{-3} torr. After deposition, GaN films were annealed at 900 °C in the pure N_2 atmosphere for the comparison purpose.

The microstructure of GaN films was studied by X-ray diffraction (XRD, D8 Discover, Bruker). The angle of X-ray incidence was 1°. The root-mean-square (*rms*) value of roughness and surface topography of the GaN films were measured by atomic force microscopy (AFM, Dimension Icon, Bruker). A field-emission scanning electron microscope (SEM, JSM-6500F, JEOL) was used to observe the surface morphology and cross-sectional images of GaN films. The compositions of GaN films were investigated with an energy dispersive spectrometer (EDS JSM-6500F, JEOL). The Hall effect measurement system (HMS-2000, Ecopia) with a maximum magnetic field of 0.51 T was used to measure the carrier concentration, mobility, and electrical conductivity for the GaN thin films. All the samples used for Hall effect measurements at room temperature had four electrical contacts made of silver paste, which were dried in an oven at 100 °C for 10 min. The absorption spectra for the GaN thin films deposited on glass substrates were measured by Ultraviolet–Visible (UV–Vis) spectrometer (V-670, Jasco) at room temperature.

3 Results and discussion

Figure 1 shows the XRD patterns for the GaN thin films deposited on Si (100) substrates at 100–400 °C by RF reactive sputtering process of technique. The XRD results indicated that the GaN films possess a wurtzite crystalline structure. When the deposition temperature was at 100 °C, the grown GaN film on Si substrate was polycrystalline.

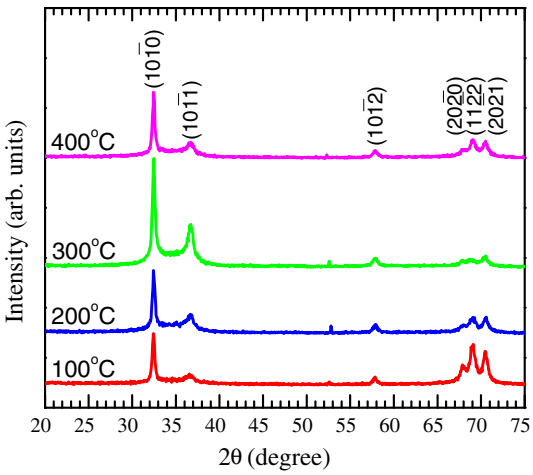

Fig. 1 XRD patterns of the GaN films deposited at 100–400 °C substrate temperature

The dominant peak in the XRD patterns observed at $2\theta = 32.45°$ was found to demonstrate a preferential growth orientation in the nonpolar crystalline plane *m*-(10–10). The other diffraction peaks observed at $2\theta = 36.32°$, 57.31°, 67.66°, 68.74°, and 70.15° were formed due to the reflection form the (10–11), (10–12), (20–20), (11–22), and (20–21) crystal planes, respectively. As the deposition substrate temperature increased from 200, 300, to 400 °C, the GaN peak positions of the (10–10) plane located at 32.45°, 32.50°, and 32.45°, respectively, remained almost unchanged, which meant that its lattice dimensions did not change with these deposition temperatures. The full width at half the maxima (FWHM) for the (10–10) peaks at $2\theta = 0.336°$, 0.334°, 0.338°, and 0.332° corresponded to the GaN films deposited at 100, 200, 300 and 400 °C, respectively. The GaN films deposited at different substrate temperature showed close quality in crystallinity. Similar diffraction behavior was observed for the GaN thin films deposited on (0001) sapphire substrates. The GaN films deposited by magnetron sputtering have shown a preferential *m*-(10–10) crystalline plane. Epitaxial GaN films grown on sapphire (0001) by MOCVD have been commercially available [12]. Their epitaxial growth for the GaN thin films by MOCVD has been conducted at high growth temperature and low growth rate. Our lower sputtering temperature does not provide sufficient kinetic energy for growing the epitaxial GaN films. Surface energy of the GaN crystal planes has been reported to be 118 meV/Å^2 for the (10–10) crystalline plane and 125 meV/Å^2 for the (0001) plane [13]. To minimize the total free energy of the deposited GaN films, our sputtered films have chosen the the (10–10) crystalline plane as the preferential growth plane. No diffraction peaks were observed due to the metallic Ga phase. Shinoda et al. [14]

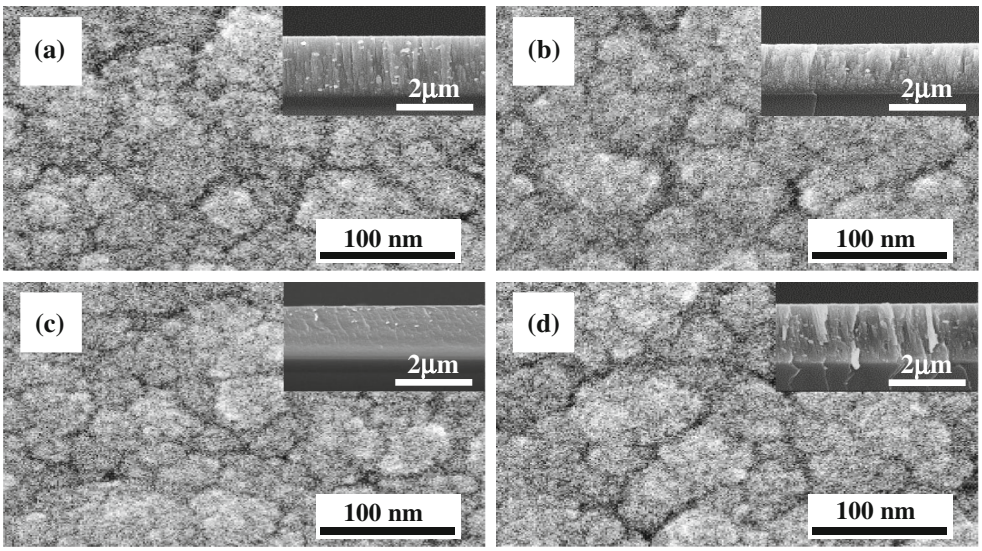

Fig. 2 SEM surface morphologies of the GaN films deposited at **a** 100 °C, **b** 200 °C, **c** 300 °C, and **d** 400 °C. The *insets* are the corresponding cross-sectional images

observed that GaN films deposited in pure N_2 atmosphere instead of the (Ar + N_2) atmosphere showed poor crystallinity. The comparative result explains the advantage of adding argon into the N_2 sputtering environment.

Figure 2 shows SEM surface morphology of the GaN films deposited at 100, 200, 300, and 400 °C on Si substrates. The images for the cross-sectional view for the films are shown as insets in the figure. The microstructure for the as-deposited GaN films show continuous, smooth, and cracks-free with no clear differences. The average grain size for all the GaN films is around 27 nm with almost similar size values. The substrate temperature did not show an observable effect on the films microstructure. As observed from the images for the cross-sectional view (the insets in Fig. 2), all the GaN films show a close thickness value around 1.5 μm and they adhere well to the Si substrates without pores or the delamination at the GaN–Si interface. Thick GaN films around 1.5 μm film thickness were grown in 90 min deposition time. The GaN films show a columnar orientation microstructure due to the preferential growth with the (10–10) plane.

Surface topographies of GaN films were investigated by AFM to obtain the *rms* value of surface roughness. Figure 3 shows the surface topographies of the GaN films grown at 100–400 °C substrate temperatures. The *rms* roughness values were found to be: 1.12, 1.07, 0.88, and 0.86 nm for the deposition substrate temperatures at 100, 200, 300, and 400 °C, respectively. The higher substrate temperature provides the sputtered GaN molecules with higher kinetic energy in order to migrate on the Si substrates and enhance the formation of smooth GaN films surface. It is known that the GaN films deposited on ZnO buffered layer by RF sputtering technique have a low *rms* value of about 0.7 nm. While GaN films grown by MOCVD method has an *rms* roughness value of around 0.5–3 nm [11, 15, 16]. The *rms* value for our film surface roughness is comparable to the published values.

The carrier concentration (n), mobility (μ), and electrical conductivity (σ) of the as-grown GaN films were plotted in Fig. 4. All the GaN films had *n*-type semiconductor properties. The electron concentrations (n_e) were 9.61×10^{18}, 3.07×10^{18}, 1.41×10^{18}, and 1.04×10^{18} cm^{-3}, at the deposition temperatures of 100, 200, 300, and 400 °C, respectively. The value of n_e decreases with increasing in substrate temperature. The change in carrier concentration is related to the change in defect concentration. From the EDS compositional analysis, the GaN films were nitrogen deficient and had the N/Ga ratios of 0.82, 0.83, 0.85, and 0.94 at the deposition temperatures of 100, 200, 300, and 400 °C, respectively. The GaN films become nitrogen deficient at lower substrate temperature and are close to be stoichiometric at higher temperature. The nitrogen vacancy (V_N) has been proposed as the dominant defect in GaN with a much shallow donor level [17–19]. The 100 °C-deposited GaN thin film with a lower N/Ga ratio of 0.82 has higher V_N defect concentration and higher electron concentration of 9.61×10^{18} cm^{-3}. The value of mobility was increased from 2.6 to 7.1 $cm^2\ V^{-1}\ s^{-1}$ as the deposition substrate temperature increased from 100 to 400 °C. The increase in mobility can be attributed to the lower electron scattering for the 400 °C-deposited GaN film with a lower n_e value. The other possible explanation can be the decreased

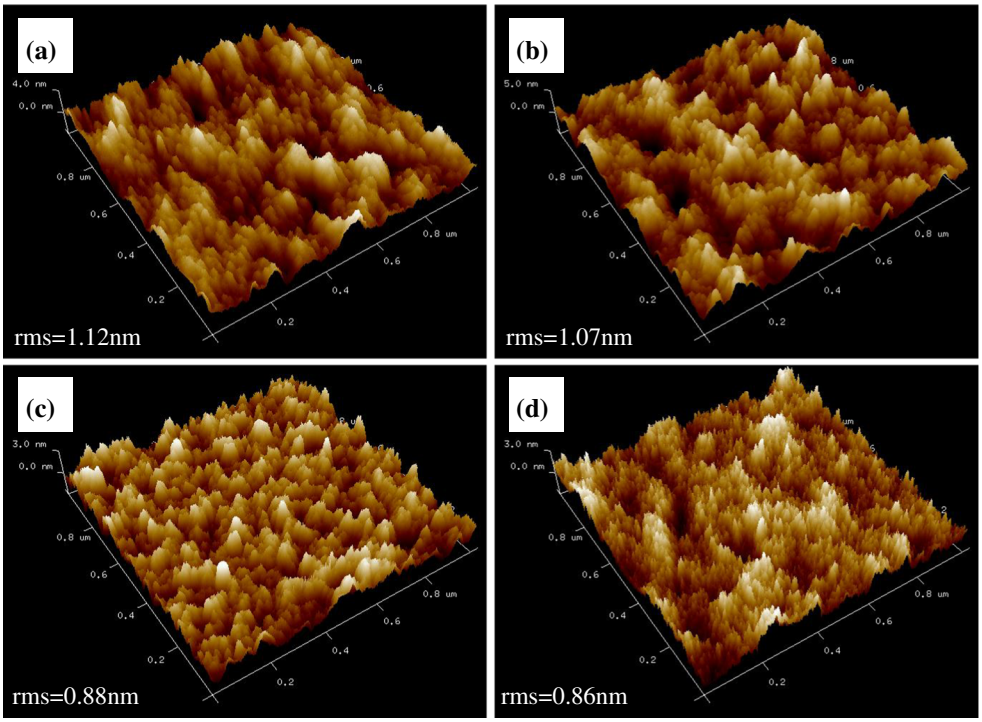

Fig. 3 AFM topographies of the GaN films deposited at **a** 100 °C, **b** 200 °C, **c** 300 °C, and **d** 400 °C substrate temperature

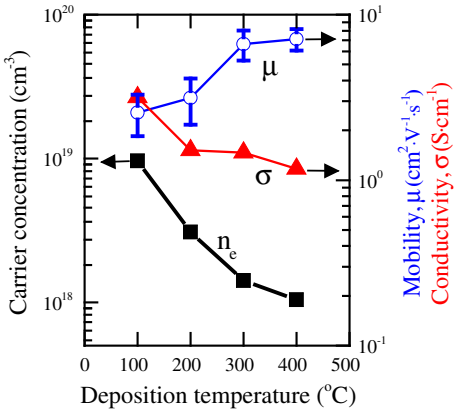

Fig. 4 Electrical properties of carrier concentration, mobility, and electrical conductivity of the GaN films grown at different deposition temperatures

concentration of the defect complexes or defect associates due to the higher growth temperature. For electrical conductivity, it is related to the product of carrier concentration and mobility and it leads to the decrease from 3.2 to 1.2 $S{\cdot}cm^{-1}$ with increasing the substrate temperature from 100 to 400 °C.

For the UV–Vis absorption measurement, GaN films were deposited on the transparent glass substrates for measuring its energy bandgap (E_g). From the UV–Vis measurements, we could calculate E_g of GaN by using the Tauc equation below [20]:

$$(\alpha h\upsilon)^2 = A(h\upsilon - E_g)$$

where α is absorption coefficient, *A* a constant, and hυ the incident photon energy. The energy bandgap of GaN films can be obtained by plotting $(\alpha h\upsilon)^2$ versus hυ and extrapolating the linear part of this $(\alpha h\upsilon)^2$–hυ plot. The absorption spectra and the extrapolation lines have been shown in Fig. 5. The E_g values were 2.97, 2.99, 3.03, and 3.06 eV for the sputtered GaN films grown at 100, 200, 300, and 400 °C substrate temperatures, respectively. All the energy bandgap values were smaller than 3.4 eV for the typical GaN. There are not many reports to have pure GaN films with an E_g value of ~3.0 eV. Knox-Davies et al. [21] showed Eg of 3.06 eV for their sputtered GaN films with the photoluminescence technique and their value increased to 3.64 eV after hydrogenation. Our small E_g value is related to the existing intrinsic defects. Van de Walle and Neugebauer, Saarinen et al., and Oila et al. [22–24] have studied about the intrinsic defects in GaN. Ga vacancy has always been mentioned for *n*-type GaN. However, nitrogen vacancy also has been proposed as the dominant defect in GaN with a much shallow donor level [17–19]. Ga vacancy in the neutral charge state is a triple acceptor with a set of levels ranging from 0.2 to 1.1 eV above the valence band edge. Other than Ga and nitrogen vacancies, the antisite and interstitial defects behave as the deep traps and do not contribute to the measured E_g values [25]. Our sputtered GaN films prepared under a plasma condition instead of a

stable thermal equilibrium condition can be the highly compensated semiconductor and its Ga vacancy exists together with the dominant nitrogen vacancy. Therefore, the smaller energy bandgap extracted from the absorption spectra can be originated from the donor–acceptor absorption. Other possible explanations are related to the existing residual stress between GaN and glass substrate and the defect-related lattice distortion. Based upon the potential fluctuation model, it is known that the distortion in crystalline orientation causes the effective bandgap dispersion and thus creates lateral potential fluctuations. Vacancies, impurities, dangling bonds, strain, and structural defects all introduce these fluctuations [26, 27].

The GaN films were tested for its thermal stability at 900 °C annealing temperature for 1 h deposition time in pure nitrogen atmosphere. Figure 6 shows SEM surface images of the annealed GaN films deposited on Si substrates. The thermal expansion coefficients of GaN and Si are 5.59×10^{-6} and 3.59×10^{-6} K^{-1}, respectively [28]. After high temperature annealing, GaN should generate tensile thermal stress due to its larger thermal expansion coefficient (α). The tensile stress can be estimated by $\Delta\alpha \times \Delta T \times E_{GaN}$, where $\Delta\alpha$ represents for the difference in α between GaN and Si, ΔT is $\sim$875 °C for temperature difference, and E_{GaN} for Young's modulus and is $\sim$200 GPa for GaN. The tensile thermal stress is about 350 MPa, which is close to the fractural strength of GaN films [29]. Although a high residual tensile stress exists in the GaN film, but this film is free of cracking. Each insert in Fig. 6 shows the cross-sectional image for the corresponding annealed film. These images were also used to examine the interfacial integrity. Obviously, there was no interfacial delamination after high temperature annealing at 900 °C.

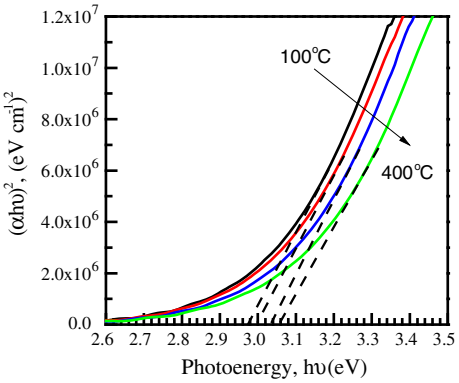

Fig. 5 Plots of $(\alpha h\upsilon)^2$ versus photon energy ($h\upsilon$) for the optical bandgap determination of the GaN films deposited at 100–400 °C substrate temperature

Electrical properties of the 900 °C-annealed GaN films were also investigated. The data were plotted in Fig. 7. After annealing at 900 °C, electrical conductivity of the GaN films changed from 3.2 S cm^{-1} for the 100 °C-deposited to 1.2 S·cm^{-1} for the 400 °C-deposited. Electrical conductivities are close for the as-deposited and annealed GaN films. However, the carrier concentration and mobility had a larger change after annealing. The carrier concentration of all annealed GaN films had increased to $\sim 10^{19}$ cm^{-3}. After annealing, the value of mobility decreased from 1.8 cm^2 V^{-1} s^{-1} for the 100 °C-deposited to 0.68 cm^2 V^{-1} s^{-1} for the 400 °C-deposited. The values of mobility for the annealed GaN films were lower than those of the as-grown films, ranging from 2.6 to 7.1 cm^2 V^{-1} s^{-1}. Therefore, annealing at 900 °C does have effects on microstructure and defect state, which lead to the changes in n_e, μ, and electrical conductivity. Our

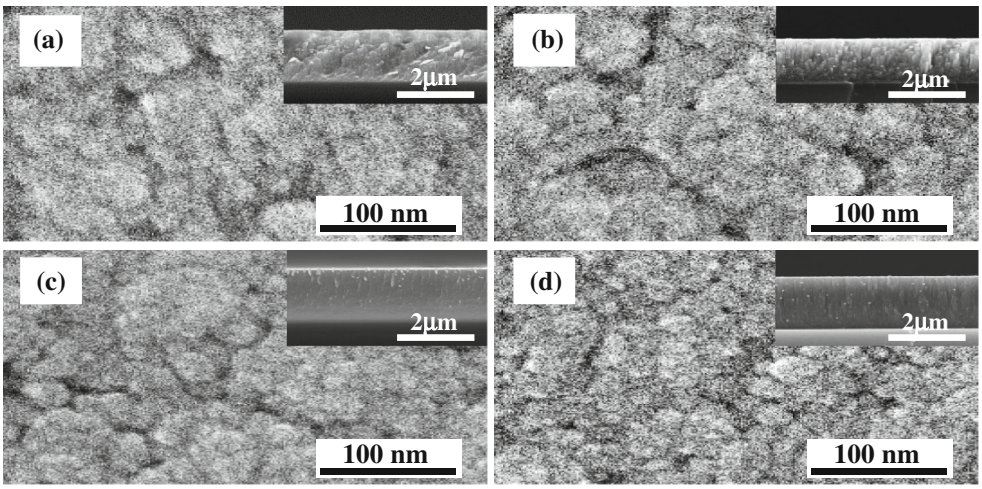

Fig. 6 SEM surface morphologies of the GaN films deposited at **a** 100 °C, **b** 200 °C, **c** 300 °C, and **d** 400 °C, followed by annealing at 900 °C in pure N_2 atmosphere. The *insets* are the corresponding cross-sectional images

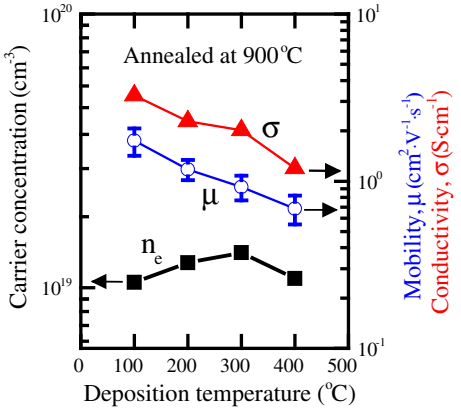

Fig. 7 Electrical properties of carrier concentration, mobility, and electrical conductivity of the GaN films deposited at different deposition temperatures, followed by annealing at 900 °C in pure N_2 atmosphere

explanation for the electrical properties of the annealed GaN thin films is related to the incorporation of oxygen impurity. The oxygen-to-nitrogen defect has been mentioned to be one of the major *n*-type defects [30, 31]. With the incorporation of oxygen, more oxygen-to-nitrogen antisite donors can increase the n_e value. The decrease in mobility can be related to the enhanced scattering from the oxygen impurity and the higher electron concentration.

4 Conclusions

GaN films were successfully deposited on Si (100) substrate at 100–400 °C substrate temperature by RF reactive sputtering with single (Ga + GaN) cermet target. This target was made by hot pressing the mixed powders of metallic Ga and ceramic GaN, not solely using the viscous Ga and the hard-to-sintered GaN. The higher deposition substrate temperature for growing the GaN films has led to the film composition close to the GaN stoichiometry, a smoother surface, the lower electron concentration of 1.04×10^{18} cm^{-3} for the 400 °C-deposited film, and higher mobility of 7.1 cm^2 V^{-1} s^{-1}. The lower energy bandgap of ~3.0 eV, as compared to the typical 3.4 eV for GaN, is caused by the intrinsic defects and the crystal distortion. After the thermal stability test at 900 °C in the N_2 atmosphere, the GaN films show a good stability in properties and microstructure and adhere well to Si substrate without interfacial delamination. The degradation in electrical properties of the annealed samples is related to the incorporation of the oxygen impurity.

Acknowledgment This work was supported by the National Science Council of the Republic of China under grant number NSC 102-2221-E-011-019-MY2.

References

1. S. Nakamura, T. Mukai, M. Senoh, Jpn. J. Appl. Phys. **30**, 1998 (1991)
2. T. Fujii, Y. Gao, R. Sharma, E.L. Hu, S.P. DenBaars, S. Nakamura, Appl. Phys. Lett. **84**, 855 (2004)
3. S.C. Jain, M. Willander, J. Naryan, R. Van Overstraeten, J. Appl. Phys. **87**, 965 (2000)
4. S. Rajan, A. Chini, M.H. Wong, J.S. Speck, U.K. Mishra, J. Appl. Phys. **102**, 044501 (2007)
5. S.J. Pearton, F. Ren, A.P. Zhang, K.P. Lee, Mater. Sci. Eng. R **30**, 55 (2000)
6. S. Nakamura, Jpn. J. Appl. Phys. **30**, 1705 (1991)
7. S. Kitamura, K. Hiramatsu, N. Sawaki, Jpn. J. Appl. Phys. **34**, 1184 (1995)
8. I. Akasaki, H. Amano, Y. Koide, K. Hiramatsu, N. Sawaki, J. Cryst. Growth **98**, 209 (1989)
9. S. Nonomura, S. Kobayashi, T. Gotoh, S. Hirata, T. Ohmori, T. Itoh, S. Nitta, K. Morigaki, J. Non. Cryst. Solids **198–200**, 174 (1996)
10. Z.X. Zhang, X.J. Pan, T. Wang, E.Q. Xie, L. Jia, J. Alloys Compd. **467**, 61 (2009)
11. H.W. Kim, N.H. Kim, Appl. Surf. Sci. **236**, 192 (2004)
12. A.P. Grzegorczyk, L. Macht, P.R. Hageman, J.L. Weyher, P.K. Larsen, J. Cryst. Growth **273**, 424 (2005)
13. J.E. Northrupa, L.T. Romano, J. Neugebauer, Appl. Phys. Lett. **74**, 2319 (1999)
14. H. Shinoda, N. Mutsukura, Thin Solid Films **516**, 2837 (2008)
15. B. Heying, E.J. Tarsa, C.R. Elsass, P. Fini, S.P. DenBaars, J.S. Speck, J. Appl. Phys. **85**, 6470 (1999)
16. I. Chyr, B. Lee, L.C. Chao, A.J. Steckl, J. Vac. Sci. Technol. B **17**, 3063 (1999)
17. M.G. Ganchenkova, R.M. Nieminen, Phys. Rev. Lett. **96**, 196402 (2006)
18. P. Perlin, T. Suski, H. Teisseyre, M. Leszcznski, I. Grzegory, J. Jun, S. Porowski, P. Bogusławski, J. Bernholc, J.C. Chervin, A. Polian, T.D. Moustakas, Phys. Rev. Lett. **75**, 296 (1995)
19. H.P. Maruska, J.J. Tietjen, Appl. Phys. Lett. **15**, 327 (1969)
20. S. Muthukumaran, R. Gopalakrishnan, Opt. Mater. **34**, 1946 (2012)
21. E.C. Knox-Davies, S.J. Henley, J.M. Shannon, S.R.P. Silva, J. Appl. Phys. **99**, 036108 (2006)
22. C.G. Van de Walle, J. Neugebauer, J. Appl. Phys. **95**, 3851 (2004)
23. K. Saarinen, T. Laine, S. Kuisma, J. Nissila, P. Hautojarvi, L. Dobrzynski, J.M. Baranowski, K. Pakula, R. Stepniewski, M. Wojdak, A. Wysmolek, T. Suski, M. Leszczynski, I. Grzegory, S. Porowski, Phys. Rev. Lett. **79**, 3030 (1997)
24. J. Oila, V. Ranki, J. Kivioja, K. Saarinen, P. Hautojarvi, J. Likonen, J.M. Baranowski, K. Pakula, T. Suski, M. Leszczynski, I. Grzegory, Phys. Rev. B **63**, 045205 (2001)
25. I. Gorczyca, A. Svane, N.E. Christensen, Solid State Commun. **101**, 747 (1997)
26. E. Oh, H. Park, Y. Park, Appl. Phys. Lett. **72**, 1848 (1998)
27. M.A. Reshchikov, G.-C. Yi, B.W. Wessels, Phys. Rev. B **59**, 13176 (1999)
28. S. Strite, H. Morkoç, J. Vac. Sci. Technol. B **10**, 1237 (1992)
29. J.Y. Huang, H. Zheng, S.X. Mao, Q. Li, G.T. Wang, Nano Lett. **11**, 1618 (2011)
30. C. Wetzel, T. Suski, J.W. Ager III, E.R. Weber, E.E. Haller, S. Fischer, B.K. Meyer, R.J. Molnar, P. Perlin, Phys. Rev. Lett. **78**, 3923 (1997)
31. T. Mattila, R.M. Nieminen, Phys. Rev. B **54**, 16676 (1996)